

FTIR and UV–Vis Spectroscopic Study of Interaction of 1-Butene on H–Ferrierite Zeolite

Costanza Pazè,^{*,†} Birsal Sazak,[‡] Adriano Zecchina,[†] and John Dwyer^{*,‡}

Centre for Microporous Materials, Chemistry Department, P.O. Box 88, Manchester M60 1QD, United Kingdom, and Dipartimento di Chimica Inorganica, Chimica Fisica e Chimica dei Materiali, Università di Torino, Via P. Giuria 7, I-10125, Torino, Italy

Received: June 24, 1999; In Final Form: September 8, 1999

The interaction of 1-butene with zeolite H–ferrierite has been studied at increasing temperatures (between 300 and 670 K) by using IR and UV–vis spectroscopies, with the aim to isolate in situ the species precursors to isobutene and high-temperature coke. The bimolecular mechanism of conversion of butene to isobutene on the fresh catalyst has been confirmed, since low branched C8 chains are observed. At 300 K, the main products of the interaction are the butene isomers 2-*cis*- and 2-*trans*-butene. At temperatures between 300 and 393 K, the presence of monoenic allylic carbocations is observed, and at temperatures between 473 and 573 K, neutral and carbocationic polyenes are present. At temperatures ≥ 623 K, the polyenyl unsaturated chains cyclize to form mono- and polycyclic aromatics. These experimental features are explained on the basis of mechanisms in which the protonated intermediates (formed by protonation of butene) can produce, by further reaction with butene molecules, mainly two kinds of products: (i) polyenyl allyl carbocations (by a butene hydride abstraction) and (ii) octane carbocations (by dimerization), which then evolve (by cracking) to isobutene.

Introduction

Because of the need for isobutene in the synthesis of methyltertiarybutyl ether (MTBE), the isomerization of *n*-butene to produce isobutene has been in recent years the focus of many investigations.^{1–23} This reaction proceeds with particularly high selectivity and yield over H–ferrierite,^{1,3} a zeolite with a 10-ring and an 8-ring system of channels, in which cavities of 0.6–0.7 nm in diameter are present.^{24–28} Two kinds of mechanism have been proposed, depending on whether the reaction occurs on the fresh or on the aged catalyst. On the fresh catalyst a bimolecular mechanism, involving an initial oligomerization of *n*-butene to octene (or higher olefins) followed by a second step involving the cracking of octene (or higher olefins) to isobutene, has been proposed.^{9,10} This mechanism leads to the formation of many side products, including propene, pentenes, and *n*-butane.²⁰ With time on stream, the mechanism becomes monomolecular, where the direct isomerization of *n*-butene proceeds via formation of a primary carbenium ion intermediate (a protonated cyclopropane intermediate is also involved).^{8,10} Reaction on the aged catalyst is characterized by higher yield and selectivity than on fresh catalyst. The reason for improved selectivity with time on stream has been the object of much debate, and explanations concerning the role of the coke in (a) modifying pore structure,^{5,12} (b) poisoning of nonselective and/or the strongest acid sites on the external surface,^{5,6,13,15,17} (c) modification of the active site from the acidic structural zeolitic proton to benzylic carbocations associated with coke (pseudomonomolecular mechanism),^{20,21} have been invoked. Consequently, studies of the

nature and formation of coke during the reaction are necessary to comprehend the basis for enhanced selectivity with time on stream.

A study of the species present on the catalyst at temperatures lower than that of the reaction has, to our knowledge, never been made. A study at lower temperature could, in principle, provide (i) information about the multiple steps of the reaction and (ii) information about the nature of the coke formed which is reported to increase the selectivity of the reaction. As far as (i) is concerned, steps that proceed at a very fast rate at higher temperatures might be observable at lower temperatures (low reaction rates). Moreover, although the isomerization of 1-butene to isobutene on H–Fer has been investigated using a great variety of techniques, a complete vibrational and electronic characterization is still unavailable. A comparative study using both techniques is interesting, because they are particularly sensitive to different functional groups. This study, then, concerns the reflectance FTIR and UV–vis–NIR characterization of the interaction between 1-butene and zeolite H–ferrierite at increasing temperatures, from 300 to 653 K.

Experimental Section

H–ferrierite (Si/Al ≈ 6.5 ; ammonium sample kindly supplied by BP) was prepared by heating the ammonium form of the zeolite at 723 K in a N₂ flow for 20 h. The interaction of the zeolite with 1-butene was studied by means of FTIR and UV–vis–NIR spectroscopy at temperature steps of 300, 353, 393, 423, 473, 523, 573, 623, and 673 K. FTIR spectra in the temperature range 353–393 K were collected in the transmission mode after cooling the sample (in pellet form) at room temperature, while spectra in the 423–653 K range were collected at the reaction temperatures using a Spectra-Tech HTEC 0030-103 diffuse reflectance cell (sample in powder form). Since IR reflectance spectra obtained at different temperatures are not directly comparable, a process of normalization

* To whom correspondence should be addressed. Phone: +44 161 2004528. Fax: +44 161 2367677. E-mail: John.Dwyer@umist.ac.uk. Phone: +39 011 6707537. Fax: +39 011 6707855. E-mail: zecchina@ch.unito.it.

[†] Università di Torino.

[‡] Centre for Microporous Materials.

was made at each temperature using a clean thermally activated sample of H-ferrierite for calibration. The spectra obtained after interaction with butene were then normalized.

FTIR spectra were obtained using a Nicolet 460 instrument with 2 cm^{-1} resolution. For the IR experiments each dosage of 1-butene was followed by a flow of pure N_2 to eliminate the gaseous and weakly sorbed species until stationary conditions were reached at each temperature. NIR-UV-vis spectra were obtained using a quartz cell. The cell, containing zeolite, was evacuated at 723 K and loaded with 1-butene (6.6 kPa), sealed, and transferred to the NIR-UV-vis spectrometer (Cary 5). For the NIR-UV-vis experiments, a single dose of 1-butene was used and the cell was heated at increasing temperatures and cooled to RT prior to taking spectra. High-purity 1-butene was supplied by BOC Gases and was dosed directly from a manifold permanently attached to the measurement cell.

To avoid the problems associated with IR reflectance technique in the study of zeolite powders in the region of frequencies between about 2000 and 1300 cm^{-1} (i.e., formation of a very intense false band due to a specular reflectance component), parallel experiments with a sample of H-ferrierite diluted in NaCl (1:1 ratio) were made. The results of the experiments show that, under the conditions used, even at the highest temperatures NaCl does not exchange the zeolitic protons, leaving all the spectral characteristics unaffected; at the same time, the region between 2000 and 1300 cm^{-1} (region of the $\text{C}=\text{C}$ vibration and of CH_3/CH_2 bending modes (δ)) becomes more clearly observable, because the specular reflectance (false) bands are almost completely eliminated.

Fits were made in the region between 3000 and 2800 cm^{-1} by means of the Origin 4.10 software program, to evaluate the degree of branching of aliphatic species (from the ratio $I(\text{CH}_3)/I(\text{CH}_2)$). To estimate the ratio of the extinction coefficients (ϵ) of CH_3 and CH_2 symmetric and asymmetric stretching modes (ν) of aliphatic molecules in the zeolitic sorbent (for the condensed phase a ratio $\epsilon_{\text{CH}_3}/\epsilon_{\text{CH}_2} \cong 2-3$ is reported²⁹), a preliminary fit of the components of *n*-butane and *n*-hexane adsorbed on H-ferrierite was made. The results show that, in H-ferrierite, a ratio of 2 is reasonable for the ratio $\epsilon_{\text{CH}_3}/\epsilon_{\text{CH}_2}$. In the effected fits, only four bands were considered, to simulate the bands associated with $\nu_{\text{CH}_3\text{asym}}$, $\nu_{\text{CH}_3\text{sym}}$, $\nu_{\text{CH}_2\text{asym}}$, $\nu_{\text{CH}_2\text{sym}}$ modes. This means that the components at $2910-2920\text{ cm}^{-1}$, due to Fermi resonance effects with δCH_3 , δCH_2 bending modes (often present in the hydrocarbon spectra²⁹), are ignored. This choice does not seem to affect the quality of the fits significantly and has the advantage of limiting the number of components in the fit.

Results

The results of the interaction of H-ferrierite with 1-butene are described at increasing temperatures. For the sake of brevity, results obtained at different temperatures but showing similar features are described in a parallel way.

Interaction of 1-Butene with H-Ferrierite in the Temperature Range 300–393 K. IR and NIR Regions of Frequency. The spectrum of unperturbed H-ferrierite is shown in Figure 1, line 1. The band at 3744 cm^{-1} is due to the OH stretching vibration of silanols prevalently located on external surfaces, while the band at about 3600 cm^{-1} is due to the presence of the strong Brønsted sites $\text{Si}(\text{OH})\text{Al}$. This peak is asymmetric on the low-frequency side, which implies heterogeneity of the Brønsted sites. Zhlobenko et al.^{30,31} have deconstructed this peak into four components at 3609, 3601, 3587, and 3565 cm^{-1} , assigned respectively to hydroxyls in 10-

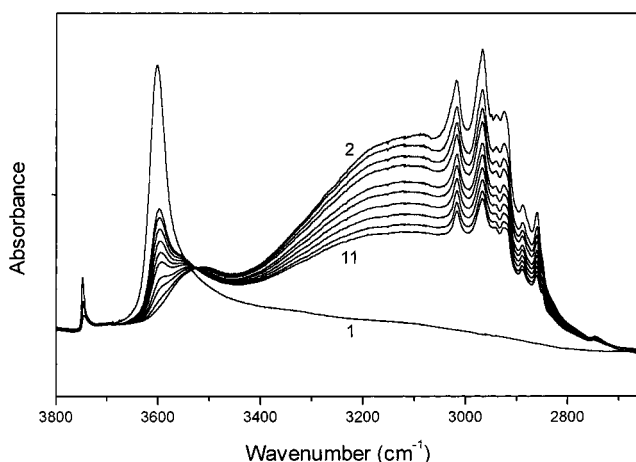


Figure 1. FTIR spectra of 1-butene sorbed on H-ferrierite at 300 K: spectrum 1, unperturbed H-FER; spectra 2–11, decreasing amounts of 1-butene (maximum pressure = 2 kPa).

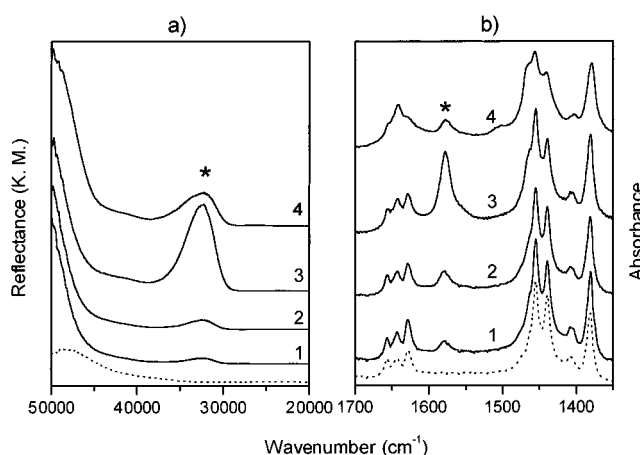


Figure 2. UV-vis (part a) and FTIR (part b) spectra of interaction of 1-butene at increasing temperatures: (1) $T = 300\text{ K}$, 15 min after interaction; (2) $T = 300\text{ K}$, after 30 min; (3) $T = 353\text{ K}$; (4) $T = 393\text{ K}$. The dotted line in part a is the UV-vis spectrum of unperturbed H-ferrierite, while the dotted line in part b is the FTIR spectrum obtained 1 min after the interaction with 1-butene. Asterisks indicate the bands which are due to the presence of monoenic carbocationic allylic species.

ring channels, in cages in 8-ring channels, in eight-membered rings, and in six-membered rings.

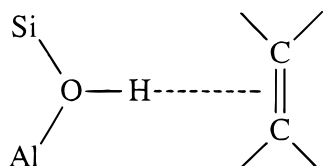
The IR spectra for the interaction of 1-butene with H-ferrierite at 300 K are shown in Figures 1 and 2b. The main features observed are as follows.

(i) The intensity of the peak with maximum at 3600 cm^{-1} , due to the unperturbed $\nu(\text{OH})$ mode of the bridged strong Brønsted groups, is reduced upon dosage of 1-butene.

(ii) Upon adsorption of 1-butene, a very broad and composite absorption between 3450 and 2600 cm^{-1} develops. A clear isosbestic point also appears at 3526 cm^{-1} , showing that a correlation between (i) and (ii) is present. The gradual erosion of the 3600 cm^{-1} peak and the formation of the broad and complex absorption in the $3450-2600\text{ cm}^{-1}$ range is associated with the formation of the hydrogen bonded species shown in Chart 1.^{32,33} A weak reversible band (νOH) is also present at about 3500 cm^{-1} , due to H-bond interaction of a residual fraction of bridged Brønsted sites with the aliphatic part of butene molecules.

(iii) In the $\nu(\text{CH})$ stretching region, bands due to νCH_2 and νCH_3 stretching modes, respectively, of the unsaturated (3016 cm^{-1} , $\nu(=\text{CH}_2)$) and saturated parts (2967 cm^{-1} , $\nu_{\text{asym}}\text{CH}_3$; 2939

CHART 1



cm^{-1} , $\nu_{\text{asym}}\text{CH}_2$; 2921 cm^{-1} , $\nu_{\text{sym}}\text{CH}_3$; 2860 cm^{-1} , $\nu_{\text{sym}}\text{CH}_2$) of (mainly) adsorbed butene molecules (complex in Chart 1) are present.

(iv) In the $1500\text{--}1350\text{ cm}^{-1}$ frequency region (Figure 2b, dotted line and curve 1), bands due to δCH_2 and δCH_3 bending modes, respectively, of the unsaturated (1410 cm^{-1} , in plane $\delta(=\text{CH}_2)$) and saturated parts (1440 cm^{-1} , $\delta_{\text{asym}}\text{CH}_3$; 1465 cm^{-1} , δCH_2 ; 1372 cm^{-1} , $\delta_{\text{sym}}\text{CH}_3$) of mainly adsorbed butene molecules (complex in Chart 1) are present.

(v) In the $\text{C}=\text{C}$ stretching region, three clearly distinguishable components are visible at 1657 , 1643 , and 1629 cm^{-1} . By comparison with low-temperature selective adsorption of 2-butene *cis-trans* isomers on other protonic zeolites,³⁴ they can be assigned respectively to the 2-*trans*-butene, 2-*cis*-butene, and 1-butene H-bond adducts with strong Brønsted sites (Chart 1). As already observed for several other adducts isolated in zeolites, these frequencies are all reduced from the gas-phase values by about $15\text{--}20\text{ cm}^{-1}$, due to weakening of the $\text{C}=\text{C}$ bond by H-bond interaction with the proton.³²

With increasing (butene) contact times (0–30 min), a band is formed at 1580 cm^{-1} (line 1, Figure 2b), and its formation is not reversible. Its presence in a region of frequency typical of aromatic ring modes cannot be explained by the formation of aromatic molecules at this low temperature (300 K), however, can be explained by the presence of allyl carbocations. In fact it has been shown from IR measurements of allyl carbocations in cryogenic superacid matrixes (supported also by *ab initio* calculations),³⁵ that allyl carbocations are characterized by a main band at about 1580 cm^{-1} ($\nu_{\text{asym}}\text{C}-\text{C}-\text{C}$). As discussed subsequently, the presence of allylic carbocations is also revealed by UV-vis spectra.

(vi) In the NIR region of frequency (Figure 3), two main bands are present in the unperturbed zeolite, at 7048 and 4656 cm^{-1} , due respectively to overtone, $2\nu(\text{OH})$, and combination, $\nu(\text{OH}) + \delta(\text{OH})$, modes of bridged strong Brønsted sites. From the frequency values for these modes, observed in the mid-IR region, the average $\delta(\text{OH})$ in plane mode of bridged hydroxyls in H-ferrierite is estimated to be at about 1050 cm^{-1} . Upon sorption of 1-butene the bands at 7048 and 4656 cm^{-1} are almost fully consumed and new absorptions appear in the regions $5972\text{--}5563$ and $4480\text{--}4206\text{ cm}^{-1}$ due, respectively, to $2\nu(\text{CH})$ and $\nu(\text{CH}) + \delta(\text{CH})$ methyl combination modes. Finally, the bands at 4154 and 4084 cm^{-1} are tentatively assigned to vibrational combination modes of allylic carbocations. The first is assigned to combinations of components at 3117 and 1043 cm^{-1} , and the second to components at 1418 (*2) and 1267 cm^{-1} , which are reported for allylic species isolated in superacidic cryogenic matrixes.³⁵

When the system is heated at 353 K , the main difference from spectra at room temperature is a strong intensification of the component at 1580 cm^{-1} , assigned to allyl carbocations (Figure 2b, line 3). On the contrary, successive heating at 393 K reduces the intensity of this band (1580 cm^{-1}) (line 4).

UV Spectra. In studying hydrocarbon species sorbed in zeolites, it is useful to compare the information given by IR and UV-vis spectroscopy. Infrared spectroscopy is quite powerful in distinguishing different saturated functional groups,

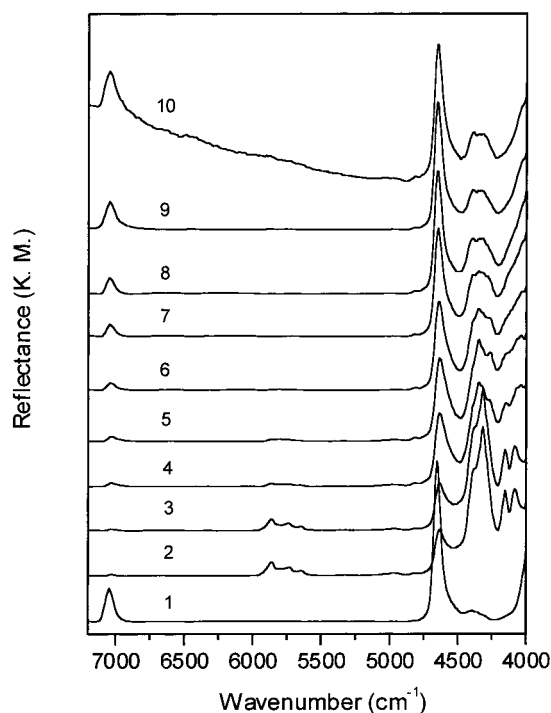


Figure 3. NIR spectra of interaction of 1-butene with H-ferrierite at increasing temperatures: (1) H-ferrierite; (2) interaction with 1-butene at 300 K ; (3) 353 K ; (4) 393 K ; (5) 423 K ; (6) 473 K ; (7) 523 K ; (8) 573 K ; (9) 623 K ; (10) 673 K .

but it gives much poorer information about molecules having a different distribution of double bonds. In this latter case, the only accessible information is present in a very limited range of frequencies (about $1500\text{--}1650\text{ cm}^{-1}$), other low-frequency molecular modes being strongly covered by the zeolitic framework bands. On the other hand, UV spectroscopy has two important advantages when dealing with double bond systems: (i) the $\pi\text{--}\pi^*$ transitions of different systems generally absorb in quite distinguishable ranges (although they can overlap); (ii) the absorption coefficients of electronic transitions of unsaturated organic compounds in the visible and near UV are usually at least 1 order of magnitude more intense than those associated with vibrational transitions.

The UV-vis spectrum of H-ferrierite is shown in Figure 2a (dotted line). By interaction with 1-butene, two bands appear at about $50\,000$ and $32\,300\text{ cm}^{-1}$. The first band is easily assigned to $\pi\text{--}\pi^*$ transitions of butene in the complex shown in Chart 1, shifted to lower frequencies with respect to the gas phase. The band centered at $32\,300\text{ cm}^{-1}$ can be assigned, by comparison with previous publications,^{36–38} to monoenic allyl carbocation species. The increase in intensity of the band at $32\,300\text{ cm}^{-1}$ is time dependent (spectra not shown for brevity). The positively charged nature of at least part of the species giving rise to this band is also confirmed by the fact that, after interaction of the system with NH_3 (a tested procedure to evidence charged species^{39,40}), the band at $32\,300\text{ cm}^{-1}$ partially disappears, since the positive charge is neutralized and the resonant system is lost.

This assignment of the band at $32\,300\text{ cm}^{-1}$ in the UV spectra strongly supports the assignment of the corresponding band at 1580 cm^{-1} in the IR (*vide supra*), since the intensities of the UV band at $32\,300$ and of the IR component at 1580 cm^{-1} increase with time at the same rate. Moreover, when the system is heated at 353 K , the intensity of the component at $32\,300\text{ cm}^{-1}$ is strongly enhanced, while subsequent heating at 393 K reduces intensity (Figure 2). This behavior is mirrored by that

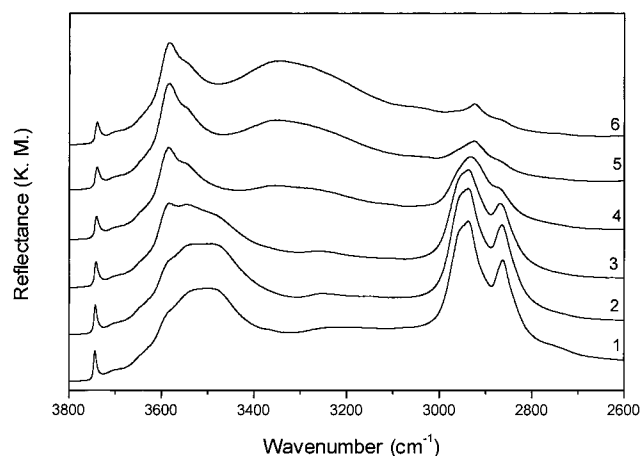


Figure 4. FTIR spectra (ν CH region) of interaction of 1-butene with H-ferrierite at increasing temperatures, after removal of physisorbed species (see Experimental Section): (1) $T = 423$ K; (2) $T = 473$ K; (3) $T = 523$ K; (4) $T = 573$ K; (5) $T = 623$ K; (6) $T = 673$ K.

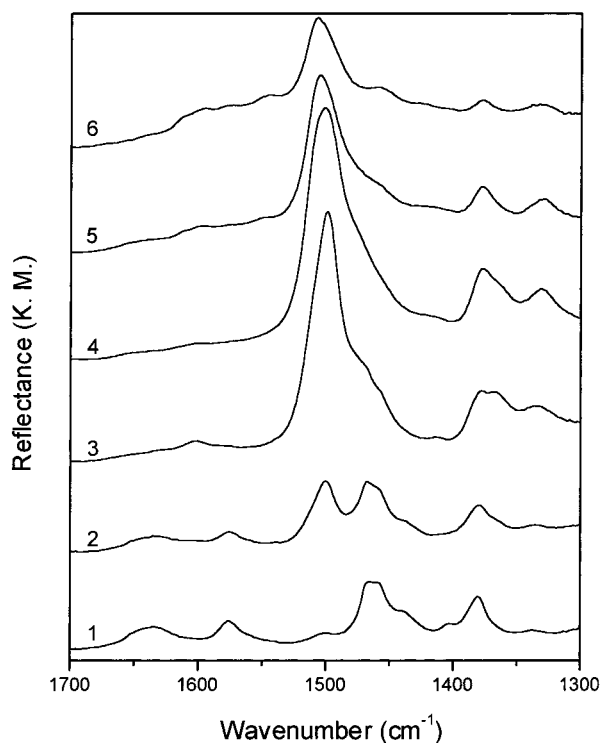


Figure 5. FTIR spectra (ν CH, ν CC region) of interaction of 1-butene with H-ferrierite at increasing temperatures, after removal of physisorbed species (see Experimental Section): (1) $T = 423$ K; (2) $T = 473$ K; (3) $T = 523$ K; (4) $T = 573$ K; (5) $T = 623$ K; (6) $T = 673$ K.

of the IR band at 1580 cm^{-1} . The presence of monoenic allyl carbocationic species in H-ferrierite is therefore revealed by the presence of bands at 32300 , 1580 cm^{-1} and is probably responsible for bands at 4080 – 4150 cm^{-1} .

Interaction of 1-Butene with H-Ferrierite at 423 K. IR and UV-Vis Regions of Frequencies. After interaction of H-ferrierite with 1-butene at 423 K (spectrum not shown for sake of brevity), the main features of the IR spectrum closely resemble those of the spectra obtained at lower temperatures. Nevertheless, after removal (under a nitrogen stream) of physisorbed species, a few important differences can be noticed (Figures 4 and 5, spectrum 1).

(i) Three components appear at 2957 , 2937 , and 2863 cm^{-1} , which are due to νCH_3 and νCH_2 asymmetric and symmetric modes in aliphatic hydrocarbons.

(ii) The band centered at about 3500 cm^{-1} , previously assigned to the interaction of a residual fraction of strong Brønsted sites interacting with the aliphatic part of butene molecules, is no longer reversible.

(iii) The intensity of the peak due to the silanols at 3744 cm^{-1} is partially decreased, and a weak adsorption is contemporarily formed at about 3700 cm^{-1} ($\Delta\nu \approx 44\text{ cm}^{-1}$).

(iv) The presence of a weak component at 1499 cm^{-1} is observed, in a region of frequencies where conjugated double bonds can absorb, presumably as a result of dehydrogenation by bimolecular hydrogen transfer.

Features (i)–(iii) can be explained by a butene protonation reaction (Chart 2). Further oligomerization reactions can occur, for example, to obtain C8 oligomers. Similar protonation reactions have already been fully studied using IR spectroscopy for interaction of olefins (ethylene and propene) with the acidic zeolites H-mordenite and H-ZSM-5, where protonation is already observed at room temperature.^{32,33} The saturated chains, obtained as products, are believed to be bonded to the zeolite by a bond having a prevalently covalent nature.⁴¹ Nevertheless, they are often represented also as ionic species since they are reported to be precursors of carbocations. The contemporary presence of long *free* saturated molecules formed after successive hydrogen transfer is unlikely, since separate experiments show that these species (up to C8) are not retained at 423 K.

Free Brønsted sites can interact with the aliphatic chains and, presumably, generate the band at 3500 cm^{-1} . The magnitude of the shift in frequency, in consequence of this H-bond interaction is, in fact, closely comparable to that of the interaction of H-ferrierite with *n*-butane (band at 3492 cm^{-1} , spectra not shown for brevity). The probability of a multiple interaction between proximate hydroxyls and a single butene molecule (such that one hydroxyl protonates the olefin and the other is H-bonded to the aliphatic chain) is enhanced by the low Si/Al ratio of the sample.

The hydrocarbon chains are located mainly inside the zeolite channels, since a difference spectrum in the region between 2000 and 1500 cm^{-1} reveals a change in the framework modes (typical of intrazeolite adsorbed molecules⁴²). The presence of some saturated hydrocarbons also on the external surface (or grown in proximity to the external mouths of the channels) is suggested by the shift in the band at 3700 cm^{-1} to 3478 cm^{-1} , due to the interaction with external silanols.

The nature of these saturated products (chain length and degree of chain branching) can be investigated by deconstruction of bands in the region 3000 – 2800 cm^{-1} , since the ratio of the integrated area (corrected by the proper extinction coefficients) of the CH_3/CH_2 bands is different in chains of different length and also for different isomers. For example, the fit at $T = 423\text{ K}$ gives a ratio ($I_{\text{CH}_3}/I_{\text{CH}_2}$) of 0.42, estimated both for the asymmetric and for the symmetric modes, which could arise from the presence of methylheptane chains. Nevertheless, it must be remembered that, as anticipated in the Experimental section, the fit in the 2880 – 2920 cm^{-1} range is not completely satisfactory because of the presence of Fermi resonance components. Moreover, even tentative assignment to chains of methyl heptane must be considered with care, because the ratio of CH_3 to CH_2 actually represents an average value for a more complex distribution of species adsorbed in the channels. What undoubtedly can be said is that the adsorbed hydrocarbons are characterized by a limited degree of branching.

The analysis of other regions of frequency in the spectra can provide additional information. Among components in the

CHART 2

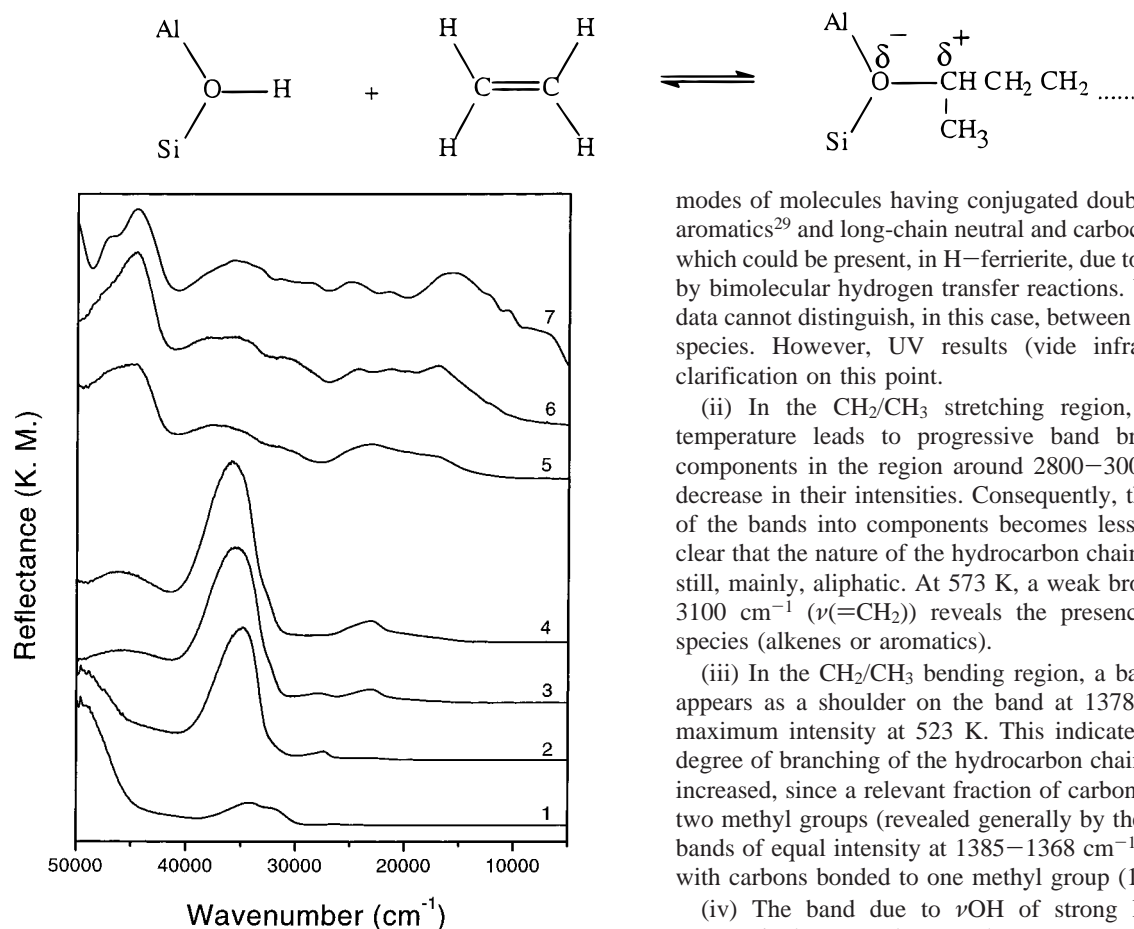


Figure 6. UV-vis spectra of interaction of 1-butene with H-ferrierite at increasing temperatures: (1) $T = 423$ K; (2) $T = 473$ K; (3) $T = 523$ K; (4) $T = 573$ K; (5) $T = 623$ K; (6) $T = 673$ K (10 min); (7) $T = 673$ K (24 h).

1500–1350 cm^{-1} range, the absorption at 1382 cm^{-1} ($\delta_{\text{sym}}\text{-CH}_3$) is particularly significant, since its position and intensity can give information about the presence of carbon atoms bonded respectively to one, two, and three methyl groups.²⁹ Since the band at 1382 cm^{-1} is slightly asymmetric on the high-frequency side, and a small shoulder at 1370 cm^{-1} is present, the carbon atoms of the sorbed hydrocarbons are predominantly bonded to one methyl group (C-CH_3), coexisting with a minor fraction of atoms bonded to two methyl groups. This result is in agreement with the result for the deconstruction of the bands for the stretching modes. Products of the protonation reaction are, therefore, mainly unbranched or slightly branched “saturated” octanes.

The corresponding UV-vis spectrum is shown in Figure 6, curve 1. The intensity of the band at 32 300 cm^{-1} , due to carbocationic allyl groups, is much decreased with respect to the intensity at lower temperatures, while a new component appears around 34 000 cm^{-1} .

Interaction of 1-Butene with H-Ferrierite in the Temperature Range 473–573 K. IR Region of Frequencies. In this range of temperature, many modifications happen in the system as the interaction temperature is increased (Figures 4 and 5, spectra 2–4).

(i) The main feature of spectra in this temperature range is the band at 1500 cm^{-1} , already present as a shoulder at 423 K, which becomes more intense (and complex) as temperature increases. The range of frequencies is typical of $\nu\text{C-C}$ stretching

modes of molecules having conjugated double bonds, such as aromatics²⁹ and long-chain neutral and carbocationic alkenes,³⁹ which could be present, in H-ferrierite, due to dehydrogenation by bimolecular hydrogen transfer reactions. Unfortunately, IR data cannot distinguish, in this case, between all these different species. However, UV results (vide infra) provide some clarification on this point.

(ii) In the CH_2/CH_3 stretching region, the increase in temperature leads to progressive band broadening of the components in the region around 2800–3000 cm^{-1} and to a decrease in their intensities. Consequently, the deconstruction of the bands into components becomes less certain, but it is clear that the nature of the hydrocarbon chains in the zeolite is still, mainly, aliphatic. At 573 K, a weak broad band at about 3100 cm^{-1} ($\nu(\text{=CH}_2)$) reveals the presence of unsaturated species (alkenes or aromatics).

(iii) In the CH_2/CH_3 bending region, a band at 1368 cm^{-1} appears as a shoulder on the band at 1378 cm^{-1} , achieving maximum intensity at 523 K. This indicates clearly that the degree of branching of the hydrocarbon chains is substantially increased, since a relevant fraction of carbon atoms bonded to two methyl groups (revealed generally by the presence of two bands of equal intensity at 1385–1368 cm^{-1} ²⁹) now coexists with carbons bonded to one methyl group (1378 cm^{-1}).

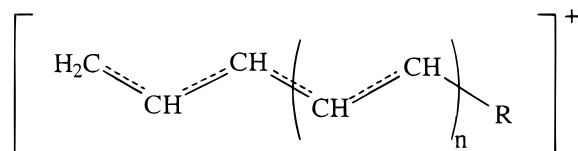
(iv) The band due to νOH of strong Brønsted sites is progressively restored, as are the NIR components at 7048 and 4656 cm^{-1} (Figure 3, spectra 6–8), while a broad band appears in the 3200–3500 cm^{-1} range.

(v) At 523 K and above, isobutene is clearly evident (νCH_2 mode at 889 cm^{-1}).

UV-Vis Region of Frequencies. The UV-vis spectra associated with the interaction of butene with H-ferrierite in the temperature range 473–573 K are strongly modified with respect to spectra at lower temperatures, in that at the higher temperature several clearly distinct components are evident (Figure 6, spectra 2–4). Two main groups of bands are present, respectively, in the 20 000–30 000 and 30 000–40 000 cm^{-1} range. Their assignment can be confidently made on the basis of numerous reported studies^{37–40,42–45} on neutral and carbocationic alkenes. It is well-known that oligomers having a different number of conjugated double bonds generate, in the electronic spectra, components at distinct frequencies. Moreover, in the UV spectra, there is greater distinction between neutral and carbocationic species, since for cations the highest of the π bonding orbitals is only half filled, and this gives rise to an allowed electronic transitions (with respect to those in neutral species) having a lower frequency.

Bands present in the 20 000–30 000 cm^{-1} are assigned to absorption by carbocationic conjugated double-bond oligomers having a different number (n) of conjugated double bonds, as shown in Chart 3. In particular, the band around 27 000 cm^{-1} (present at 473 and 523 K) is assigned to dienic ions (Chart 3, $n = 1$), while that at about 23 000 cm^{-1} (present at 523 and 573 K) is assigned to trienic ions ($n = 2$). Finally, the tail present at lower frequency (20 000–15 000 cm^{-1}) is due to species having $n > 2$. As the temperature increases, the extended double bond conjugation in species of type A also increases.

CHART 3



R = e.g. Methyl or Ethyl or H
Species A

Absorptions in the range 30 000–40 000 cm^{-1} (which consist of a band centered at about 35 000 cm^{-1} , to which large components at 36 000–39 000 cm^{-1} which merge as temperature increases) are assigned^{39,43} to neutral conjugated double bond oligomers having a different number (n) of conjugated double bonds, as shown in Chart 4.

A straightforward distinction in the assignation of the components at 35 000 cm^{-1} and 36 000–39 000 cm^{-1} cannot be made, since the nature of the alkyl substituent R is able to shift the absorption by the same order of magnitude of the frequency shifts observed.³⁹ Nevertheless, absorptions in the 35 000–40 000 cm^{-1} range are consistent with species B having a number (n) of 2 and 3 conjugated double bonds. Moreover, the assignment is of limited certainty because of the presence of a broad absorption at 40 000–50 000 cm^{-1} (vide infra).

Interaction of 1-Butene with H-Ferrierite at 623–673 K.

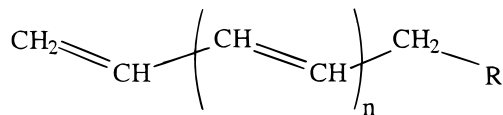
IR Region of Frequencies. The interaction of butene and H-ferrierite at 623 and 673 K (Figures 4 and 5, spectra 5 and 6) strongly modifies the spectrum with respect to spectra obtained at lower temperatures. Results at the highest temperature (673 K) reveal the following.

(i) In the νCH region, vibrational modes due to long aliphatic chains are not evident. Three components, at 2921, 2865, and 3070–3000 cm^{-1} , appear and can be attributed to the presence of aromatics (CH stretching at 3070–3000 cm^{-1}) substituted by methyl groups (2921 cm^{-1} (sym. νCH_3), 2865 cm^{-1} (2 asym. δCH_3)).

(ii) A complex absorption is generated between 1350 and 1650 cm^{-1} . In addition to the weak components due to CH_3/CH_2 bending modes at 1462 and 1379 cm^{-1} , absorptions at 1617, 1601, 1580, 1551, 1511, and 1427 cm^{-1} are also evident. These bands can all be attributed to the presence of an extremely heterogeneous group of alkylated aromatic molecules (for example *o,m,p*-xylene and toluene, but also to polycyclic molecules). Andy et al.²² report a series of polycyclic aromatics observed in the coke extracted from the zeolite. At this stage, a further assignment of IR frequencies is not possible; however, the extremely low intensity of the bands associated with νCH vibrations with respect to that for νCC modes suggests the presence of condensed rings.

(iii) The strong Brønsted sites are partially and irreversibly consumed, and a broad band is formed between 3500 and 3100 cm^{-1} . These two phenomena are strongly correlated since further dosage of 1-butene causes their progressive enhancement (spectra not shown for brevity). Since the frequency shift is similar to that obtained with aromatic molecules,⁴⁶ the band at 3500–3100 cm^{-1} can be attributed to hydrogen bonding interaction between strong Brønsted sites and the aromatic species forming the coke. This means that part of the coke is certainly present in the internal surface regions, and this is confirmed by the slight modification of framework combination

CHART 4



R = e.g. Methyl or Ethyl or H
Species B

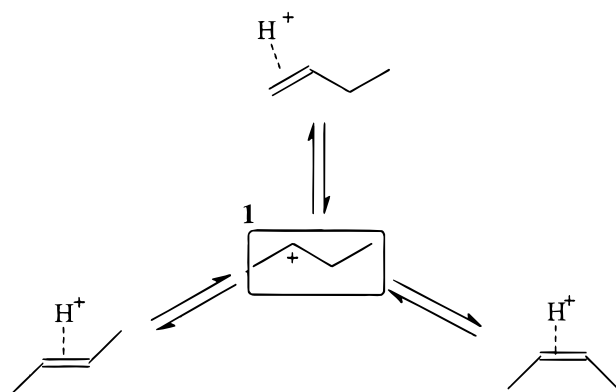
modes between 2100 and 1700 cm^{-1} (spectra not shown for brevity).⁴⁷ Finally, it should be noticed that the band at 3500–3100 cm^{-1} cannot be also attributed to isobutene molecules remaining trapped within the smaller channels, even though this might result in a similar shift of frequency, because no other bands typical of isobutene are observable.

UV region of Frequencies. UV spectra obtained at 623 and 673 K (Figure 6, spectra 5–7) are mainly characterized by three groups of absorptions, at 42 000–50 000, 27 000–42 000, and 5000–27 000 cm^{-1} , respectively; the well-defined strong component observable, at lower temperatures, in the 30 000–40 000 cm^{-1} range (vide supra), is not evident. The complexity of the spectra reveals, as in the case of the IR spectra, a considerable number of hydrocarbon species, both neutral and carbocationic, having aromatic character. Since the electronic properties of aromatic and polycyclic molecules in superacidic environments are partially known,⁴⁸ a general assignment of the components can be given, but a precise assignment is not possible, due to the contemporary presence of neutral and carbocationic species. For example, it seems clear that, for each aromatic molecule, two kinds of carbocation can be formed either as a result of hydride ion abstraction from the side chain or by a proton attack on the ring. Carbocationic and neutral aromatic molecules can be characterized by electronic absorptions separated by 15 000–20 000 cm^{-1} . For example, the benzyl ion (carbocation of toluene) absorbs UV radiation at about 22 000 cm^{-1} ,⁴⁹ while the lower energy absorption of toluene is present at 38 000 cm^{-1} .⁵⁰

Whereas absorptions at highest energies (42 000–50 000 cm^{-1}) can be easily assigned to neutral molecules having a single aromatic ring (alkylated benzenes), absorptions in the region between 40 000 and 20 000 cm^{-1} can be assigned to carbocationic and neutral (the high-frequency part) species (aromatics but also linear) having an extensive conjugated double bond system (e.g., molecules having six condensed rings are characterized by a low-frequency energy at 20 000 cm^{-1}). As the frequency of the electronic transition decreases, the number of aromatic condensed rings increases.⁵⁰ Prolonged heating at 670 K (24 h, spectrum 7, Figure 6) leads to an increase of the intensity of the components in the region between 35 000 and 5000 cm^{-1} , which indicates highly polycyclic graphitic-like coke.

These results are in accord with those obtained by Andy et al.,²² who studied the composition of high-temperature coke after destruction of the catalyst with HF and successive extraction of carbon species by methyl chloride; nevertheless, this method could not differentiate between neutral and charged aromatics. In our experiments, the carbocationic nature is confirmed by the dosage of NH_3 on the coked system: all bands in the 40 000–5000 cm^{-1} range are then subjected to a partial decrease of intensity.

CHART 5



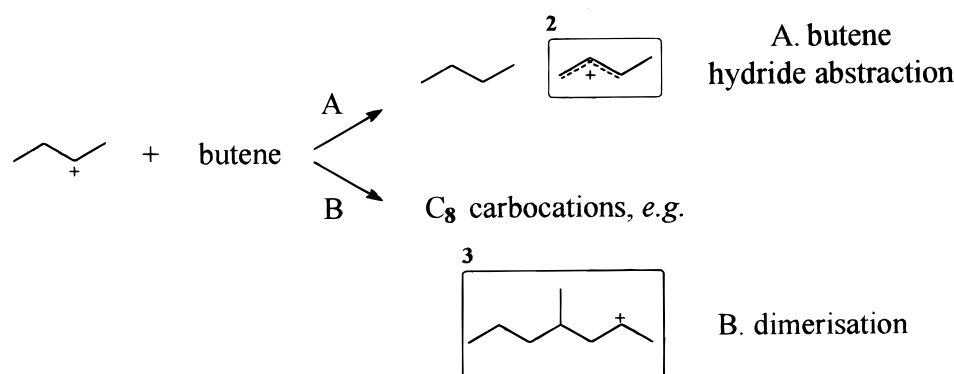
Discussion

Coke, together with isobutene (plus small amounts of C2–C5 species), is the main product of interaction of 1-butene with H–ferrierite. Moreover, it is known that the influence of coke on the isobutene selectivity of the system is of great interest. Whereas the mechanisms of isobutene formation on fresh and aged catalysts have been extensively studied, no general scheme including the competitive reactions of coke and isobutene formation has been fully developed.

The interaction of butene and H–ferrierite at increasing temperatures is studied here with the aim to identify the precursors of coke. The identification of coke precursors using this procedure is strengthened by the clear correspondence of the IR and UV spectra obtained after interaction of butene at increasing steps of temperature, and after prolonged interaction at the maximum temperature (spectra not shown for sake of brevity). From the obtained spectroscopic data, the precursors of isobutene and of aromatic high temperature coke can be schematically distinguished as formed during four different phases.

(i) Protonation of Butene. The formation of *cis*- and *trans*-2-butene ($\nu_{C=C}$ modes at 1657 and 1643 cm^{-1}) is observed after interaction with 1-butene at room temperature. The double bond migration of olefins is known to be catalyzed by Brønsted sites. Either in acid solutions or in acid zeolites, reaction proceeds (unless at very low temperatures³⁴) via protonated intermediates, according to Chart 5. On H–ferrierite, isomerization of the double bond is evident at 300 K, which means that, at this temperature, the corresponding protonated intermediates (species 1 in Chart 5), even if not directly visible in the infrared (their vibration modes being covered by those of butene gas), are also formed, or at least can exist as an excited state. In Chart 5, the interaction of the zeolitic proton with the olefins is indicated by $H^+\cdots$.

CHART 6



Protonation of butene is a reversible step, since at 300 K an outgassing procedure does not lead to the appearance of the modes typical of saturated groups of species 1 (2800–3000 cm^{-1} , see Figure 1). Evidently, the butene molecules interact with all the strong Brønsted sites, located either in 10- and 8-ring channels (complete consumption of the band at 3600 cm^{-1} , Figure 1).

(ii) Formation of Monoenic Allylic Cationic Species. The formation at low temperatures (between 300 and 393 K) of monoenic allylic cationic species is observed by both UV–vis and IR spectroscopy (bands at 32300 and 1580 cm^{-1}). The formation of these monoenic allyl groups (species 2 in Chart 6) could be due to the reaction of charged complexes 1 with further *n*-butene molecules (1-butene and *cis*- and *trans*-2-butene), via hydride abstraction from butene. Butane is presumably formed in parallel from species 1, according to reaction A shown in Chart 6; the formation of butane has been in fact reported.²⁰ The formation of species 2 is a slow, but irreversible, reaction at room temperature, and a maximal concentration is observed at 353 K. At higher temperatures (393–423 K), it is still observable but in reduced amount.

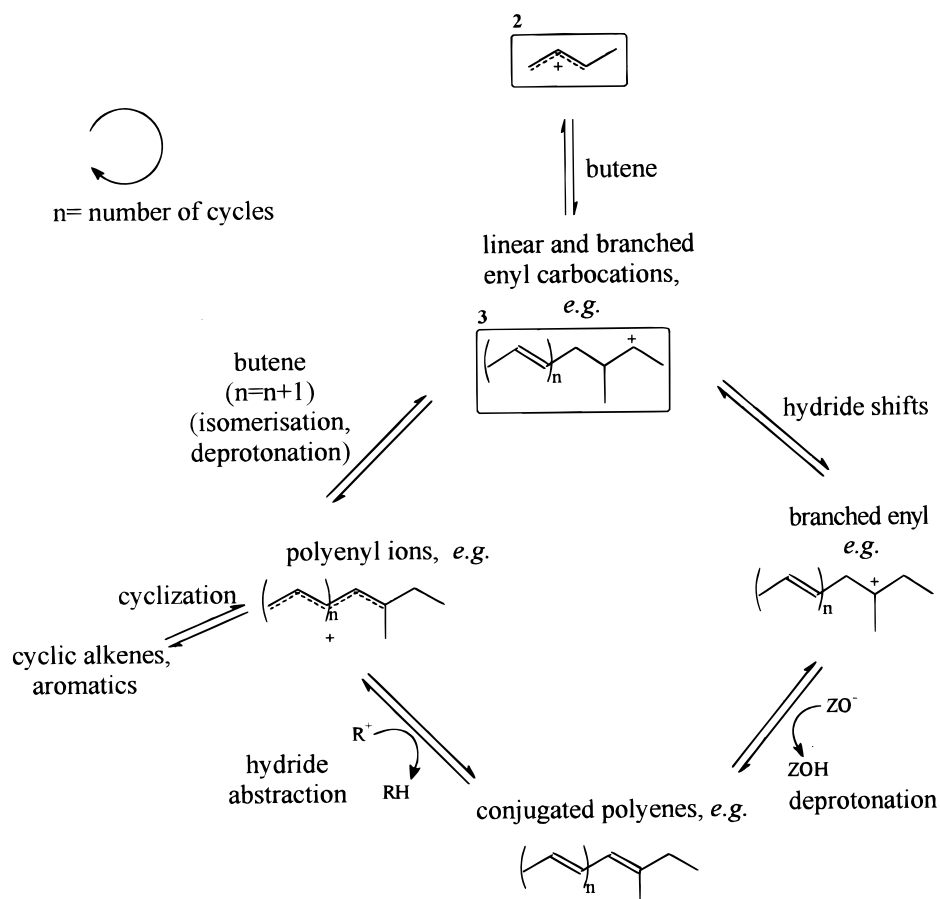
(iii) Dimerization of Butene. According to Guisnet⁹ and Meriaudeau,¹⁰ isobutene is formed, over fresh catalyst, by dimerization of two butene molecules (according to path B of Chart 6) to form C₈ molecules. Further isomerization steps (alkyl shifts) lead to the more branched oligomers. Finally, cracking reactions (β scission) produce isobutene and other products. This mechanism is broadly confirmed by the present IR spectroscopic results, which indicate the formation of methylheptane carbocations in a first step (fit in the 2800–3000 cm^{-1} region) and then the increase in degree of branching, with maximum branching around 520 K, a temperature at which the first 2-alkyl-1-alkene molecules (e.g., isobutene and 2-methyl-1-pentene) are observed (band at 889 cm^{-1} , δCH_2).

These results indicate that reaction B in Chart 6 (present at temperatures higher than 300 K) is characterized by a higher activation energy than reaction A (slow conversion, at RT).

(iv) Formation of Neutral and Charged Allylic Resonant Chains. The presence of carbocationic and neutral conjugated double-bond oligomers is the more important phenomenon in the temperature range 473–573 K. A progressive lengthening of the conjugated double bond chains is observed as the temperature of interaction increases. The monoenic and polyenylic allyl cations are resonance stabilized. Their formation can be explained by multistep reactions as shown in Chart 7.

In the first step, the allylic species 2 interact with *n*-butene to form octenyl carbocations; by successive hydride shift ($\sim H$)

CHART 7



(*e.g.*, to obtain the more stable tertiary carbocations) and deprotonation (*e.g.*, by the zeolitic $SiOAl^{δ-}$ group, represented as ZO^- in Chart 7) neutral dienes can be formed. Further hydride abstraction by carbocationic species (R^+) leads to the formation of carbocationic dienes. Iteration of these steps by further reaction with butene molecules (followed by isomerization–deprotonation) gives rise to longer carbocationic allylic systems having more than three resonant double bonds. This mechanism is similar to that hypothesized for interaction of propene with H-ZSM-5 at high temperature.⁵¹

This mechanism well justifies the extensive (and apparently anomalous) decrease of intensity of the UV components at 420 K (above all around 30 000–40 000 cm^{-1}), and the successive strengthening of the intensities, in the same range of frequencies, at higher temperatures (470–670 K) (Figure 6). This feature can be explained by the transformation of species **2** ($\pi-\pi^*$ transition in the experimentally accessible UV region of frequencies) to species **3** (with $n = 1$, single double bond, so that the $\pi-\pi^*$ transition absorbs at energies higher than 50 000 cm^{-1}). Only the successive deprotonation step (see Chart 7) causes the formation of species having two or more conjugated double bonds, which absorb radiation in the studied UV region.

Finally, polyenyl ions can undergo cyclization, according to a mechanism that could be similar to that observed in acid solutions, in which 1,5-cyclization of dienylic ions has been invoked. In the present study, evidence for cyclization is first seen around 620 K and involves a large fraction of the neutral and charged polyenylic species.

It is noteworthy that all the species shown in Charts 5, 6, and 7 (except otherwise indicated) are supported by IR and/or

TABLE 1

hydrocarbons	IR (cm^{-1})	UV–vis (cm^{-1})
H-bond butenes:		50 000
1-	1629	
2- cis	1643	
2- trans	1657	
aliphatic products	2957, 2937, 2863 1378, 1368	
allyl carbocation	1580, 4154, 4084	32 300
dienyl carbenium ions	1450–1550	27 000
trieryl carbenium ions	1450–1550	23 000
enyl carbenium ions, $n \geq 3$	1450–1550	20 000–15 000
neutral di- and trienes,	1450–1550	35 000–39 000
aromatics	3000–3070, 2921, 2865, 1650–1450	50 000–10 000

UV spectroscopic observations and that their presence in particular steps of the hypothesized mechanism for coke formation is directly connected to their early or late appearance in the IR and UV–vis spectra at increasing temperatures.

Accepting the scheme in Chart 6 as a qualitative picture of the initial process, it can be suggested that path A in Chart 6 (hydride abstraction) leads mainly to the coke formation, while path B (dimerization) is responsible for the formation of isobutene (following a bimolecular mechanism on a fresh catalyst). This classification cannot, however, be considered as rigid, since for example further dehydrogenation of C8 carbocations (Chart 6, path B) would generate again the unsaturated species here classified as “coke” (Chart 6, path A). Nevertheless, it is clear that the formation of allylic positive species is the determinant step in coke formation on H-ferrierite by interaction with 1-butene and that the competition between “coke” and isobutene formation begins with the C4 charged species **1** (Chart

5), which are formed in the very early stages by interaction of strong zeolitic protons with butene.

Conclusions

The interaction of 1-butene with H—ferrierite at increasing temperatures (between 300 and 673 K) has been studied using IR and UV—vis spectroscopies. A summary of assignments is shown in Table 1. Precursors of isobutene and coke have been observed, and a mechanism is proposed to explain their presence. First of all, the bimolecular mechanism of conversion of butene to isobutene on the fresh catalyst has been confirmed, since low branched octane chains are observed. The isomerization of 1-butene (to 2-*cis*, 2-*trans*-butene) has been observed at room temperature. By reaction of the protonated intermediate with butene, two reaction paths are hypothesized: (i) a butene hydride abstraction, with formation of dienic allyl carbocations, and (ii) dimerization to form octane carbocations and (by successive cracking) isobutene. The reaction of allylic carbenium ions with butene molecules, followed by H transfer, leads to the formation of long, unsaturated, resonant neutral and carbocationic chains. At temperatures ≥ 623 K, these unsaturated chains cyclize to form mono- and polycyclic aromatics.

Acknowledgment. The Centre for Microporous Materials acknowledges EPSRC, BNFL, BOC, Engelhardt, and ICI. A. Zecchina and C. Pazè acknowledge Italian MURST support (Cofin 98, Area 03) and CNR (Project 98.01987.CT03).

References and Notes

- (1) Butler, A. C.; Nicolaides, C. P. *Catal. Today* **1993**, 18, 443.
- (2) Natarajan, S.; Wright, P. A.; Thomas, J. M. *J. Chem. Soc., Chem. Commun.* **1993**, 1861.
- (3) Mooiweer, H. H.; de Jong, K. P.; Kraushaar-Czarnetzki, B.; Stork, W. H. J.; Krutzen, B. C. H. *Stud. Surf. Sci. Catal.* **1994**, 84, 2327.
- (4) De Jong, K. P.; Mooiweer, H. H.; Buglas, J. G.; Maarsen, P. K. *Stud. Surf. Sci. Catal.* **1997**, 111, 127.
- (5) Xu, W.; Yin, Y.; Suib, S. L.; O'Young, C. J. *Phys. Chem.* **1995**, 99, 758.
- (6) Xu, W.; Yin, Y.; Suib, S. L.; Edwards, J. E.; O'Young, C. J. *Phys. Chem.* **1995**, 99, 9443.
- (7) Pellet, R. J.; Casey, D. G.; Huang, H.-M.; Kessler, R. V.; Kuhlman, E. J.; O'Young, C.-L.; Sawicki, R. A.; Ugolini, J. R. *J. Catal.* **1995**, 157, 423.
- (8) O'Young, C.-L.; Pellet, R. J.; Casey, D. G.; Ugolini, J. R.; Sawicki, R. A. *J. Catal.* **1995**, 151, 467.
- (9) Guisnet, M.; Andy, P.; Gnep, N. S.; Benazzi, E.; Travers, C. J. *Catal.* **1996**, 158, 551.
- (10) Mériaudeau, P.; Bacaud, R.; Ngoc Hung, L.; Vu, Anh. T. *J. Mol. Catal. A* **1996**, 110, L177.
- (11) Seo, G.; Jeong, H. S.; Hong, S. B.; Uh, Y. S. *Catal. Lett.* **1996**, 36, 249.
- (12) Seo, G.; Jeong, H. S.; Jang, D.-L.; Cho, D. L.; Hong, S. B. *Catal. Lett.* **1996**, 41, 189.
- (13) Xu, W.; Yin, Y.; Suib, S. L.; Edwards, J. E.; O'Young, C. J. *Catal.* **1996**, 163, 232.
- (14) Jousse, F.; Leherter, L.; Vercauteren, D. P. *Mol. Simul.* **1996**, 17, 175.
- (15) Houzvicka, J.; Ponec, W. *Ind. Eng. Chem. Res.* **1997**, 36, 1424.
- (16) Jousse, F.; Leherter, L.; Vercauteren, D. P. *J. Mol. Catal. A* **1997**, 119, 165.
- (17) Mériaudeau, P.; Naccache, C.; Le, H. N.; Vu, T. A.; Szabo, G. J. *Mol. Catal. A* **1997**, 123, L1.
- (18) Mériaudeau, P.; Tuan, V. A.; Le, N. H.; Szabo, G. J. *Catal.* **1997**, 169, 397.
- (19) Mériaudeau, P.; Tuan, V. A.; Hung, L. N.; Naccache, C.; Szabo, G. J. *Catal.* **1997**, 171, 329.
- (20) Guisnet, M.; Andy, P.; Gnep, N. S.; Travers, C.; Benazzi, E. *Stud. Surf. Sci. Catal.* **1997**, 105, 1365.
- (21) Guisnet, M.; Andy, P.; Boucheffa, Y.; Gnep, N. S.; Travers, C.; Benazzi, E. *Catal. Lett.* **1998**, 50, 159.
- (22) Andy, P.; Gnep, N. S.; Guisnet, M.; Benazzi, E.; Travers, C. J. *Catal.* **1998**, 173, 322.
- (23) Wichterlová, B.; Šilková, N.; Uvarova, E.; Cejka, J.; Sarv, P.; Paganini, C.; Lercher, J. A. *Appl. Catal. A* **1999**, 182, 297.
- (24) Jin, Y. S.; Auroux, A.; Vedrine, J. C. *Appl. Catal.* **1988**, 37, 1.
- (25) Jin, Y. S.; Auroux, A.; Vedrine, J. C. *Appl. Catal.* **1988**, 37, 21.
- (26) Fjellvåg, H.; Lillerud, K. P.; Norby, P.; Sørby, K. *Zeolites* **1989**, 9, 152.
- (27) Morris, R. E.; Weigel, S. J.; Henson, N. J.; Bull, L. M.; Janicke, M. T.; Chmelka, B. F.; Cheetham, A. K. *J. Am. Chem. Soc.* **1994**, 116, 11849.
- (28) Sarv, P.; Wichterlová, B.; Cejka, J. *J. Phys. Chem. B* **1998**, 102, 1372.
- (29) Colthup, N. B.; Daley, L. H.; Wiberly, S. E. *Introduction to Infrared and Raman Spectroscopy*; Academic Press: New York, 1975.
- (30) Lukyanov, D. B.; Zholobenko, V. L.; Dwyer, J.; Barri, S. A. I.; Smith, W. J. *J. Phys. Chem. B* **1999**, 103, 8197.
- (31) Zholobenko, V. L.; Lukyanov, D. B.; Dwyer, J.; Smith, W. J. *J. Phys. Chem. B* **1998**, 102, 2715.
- (32) Spoto, G.; Bordiga, S.; Ricchiardi, G.; Scarano, D.; Zecchina, A.; Borello, E. *J. Chem. Soc., Faraday Trans.* **1994**, 90, 2827.
- (33) Geobaldo, F.; Spoto, G.; Bordiga, S.; Lamberti, C.; Zecchina, A. *J. Chem. Soc., Faraday Trans.* **1997**, 93, 1243.
- (34) Kondo, J. N.; Domen, K.; Wakabayashi, F. *Micr. Mes. Mater.* **1998**, 21, 429.
- (35) Buzek, P.; von Schleyer, R. P.; Vancik, H.; Mihalic, Z.; Gauss, J. *Angew. Chem., Int. Ed. Engl.* **1994**, 33, 448.
- (36) Deno, N. C.; Bollinger, M. J.; Friedman, N.; Hafer, K.; Hodge, J. D.; Hauser, J. J. *J. Am. Chem. Soc.* **1963**, 85, 2998.
- (37) Olah, G. A.; Pittman, C. U., Jr.; Waack, R.; Doran, M. J. *Am. Chem. Soc.* **1966**, 88, 1488.
- (38) Förster, H.; Seebode, J.; Fejes, P.; Kiricsi, I. *J. Chem. Soc., Faraday Trans.* **1986**, 83, 1109.
- (39) Bordiga, A.; Ricchiardi, G.; Spoto, G.; Scarano, D.; Carnelli, L.; Zecchina, A. *J. Chem. Soc., Faraday Trans.* **1993**, 89, 1843.
- (40) Chiappetta, R.; Bodoardo, S.; Geobaldo, F.; Fajula, F.; Garrone, E. *Res. Chem. Intermed.* **1999**, 25, 111.
- (41) Corma, A. *Chem. Rev.* **1995**, 95, 559.
- (42) Zecchina, A.; Geobaldo, F.; Spoto, G.; Bordiga, S.; Ricchiardi, G.; Buzzoni, R.; Petrini, G. *J. Phys. Chem.* **1996**, 100, 16584.
- (43) Knoll, K.; Schrock, R. R. *J. Am. Chem. Soc.* **1989**, 111, 7989.
- (44) Deno, N. C.; Pittman, C. U., Jr.; Turner, J. O. *J. Am. Chem. Soc.* **1965**, 87, 2153.
- (45) Sorensen, T. S. *J. Am. Chem. Soc.* **1965**, 87, 5075.
- (46) Liao Su, B.; Barthomeuf, D. *J. Catal.* **1993**, 139, 81.
- (47) Zecchina, A.; Geobaldo, F.; Spoto, G.; Bordiga, S.; Ricchiardi, G.; Buzzoni, R.; Petrini, G. *J. Phys. Chem.* **1996**, 100, 16584.
- (48) Olah, G. A.; Schleyer, R. P. *Carbonium Ions*; Wiley-Interscience: New York, 1968; Vol. 1.
- (49) Förster, H.; Kiricsi, I.; Tasi, G. *J. Mol. Struct.* **1993**, 296, 61.
- (50) Rao, C. N. R. *Ultraviolet and visible spectroscopy*, 2nd ed.; Butterworth: London, 1967.
- (51) Kiricsi, I.; Förster, H. *J. Chem. Soc., Faraday Trans.* **1988**, 84, 491.